

and theoretical studies revealed that noncollinear spiral spin structures breaking the spatial inversion symmetry often make the system ferroelectric. A 120° structure which is the classical ground state in a Heisenberg triangular lattice antiferromagnet (TLA) also breaks the inversion symmetry, being another candidate for inducing ferroelectricity. To test this prediction, we investigated magnetic and dielectric properties of a typical TLA  $\text{CuCrO}_2$  showing the 120° structure with easy axis anisotropy [1]. Single crystals of  $\text{CuCrO}_2$  were successfully grown by a flux method. Temperature profile of the magnetic susceptibility shows an anomaly at  $T_N \approx 24.5\text{K}$ , due to the ordering into the 120° structure. Dielectric constant perpendicular to the  $c$  axis shows a sharp peak near  $T_N$ . In addition, spontaneous polarization perpendicular to the  $c$  axis emerges below  $T_N$ . The sign reversal of spontaneous polarization by applying electric field is also observed below  $T_N$ . These results ensure the emergence of ferroelectricity induced by 120° structure in  $\text{CuCrO}_2$ . Furthermore, the ferroelectric property is affected by an application of magnetic fields. In the presentation, we show detailed experimental results, and discuss the coupling between the magnetic and dielectric properties in the TLA  $\text{CuCrO}_2$ .

[1] H. Kadowaki, H. Kikuchi and Y. Ajiro, *J. Phys.: Condens. Matter* 2, 4485 (1990)

Keywords: strongly correlated systems, magnetoelectricity, magnetic frustration

## P08.14.146

*Acta Cryst.* (2008). A64, C463

### Location of proton in proton conducting perovskite oxides $\text{Ba}_3\text{Ca}_{1.18}\text{Nb}_{1.82}\text{O}_{8.73}$ and $\text{BaZr}_{0.8}\text{Sc}_{0.2}\text{O}_{2.9}$

Hitoshi Kawaji<sup>1</sup>, Tomotaka Shimoyama<sup>1</sup>, Tooru Atake<sup>1</sup>, Hiroshi Fukazawa<sup>2</sup>, Naoki Igawa<sup>2</sup>

<sup>1</sup>Tokyo Institute of Technology, Materials and Structures Laboratory, 4259 Nagatsuta-cho, Midori-ku, Yokohama, Kanagawa, 226-8503, Japan, <sup>2</sup>Japan Atomic Energy Agency, 2-4 Shirane Shirakata, Tokai-mura, Nakagun, Ibaraki, 319-1195, Japan, E-mail: kawaji@msl.titech.ac.jp

Some oxides with perovskite structure have high proton conductivity of  $10^{-2}$  -  $10^{-3}$   $\text{Scm}^{-1}$ . However, the locations of proton, the proton conduction path, and the thermodynamic properties have not been clarified yet. In the present study, the location of proton and the lattice vibrations have been studied by neutron diffraction and heat capacity measurements. The samples of a proton conducting mixed perovskite oxide  $\text{Ba}_3\text{Ca}_{1.18}\text{Nb}_{1.82}\text{O}_{8.73}$  and a simple perovskite oxide  $\text{BaZr}_{0.8}\text{Sc}_{0.2}\text{O}_{2.9}$  were synthesized by a method of solid-state reaction. The neutron diffraction experiments were performed using HRPD at JAEA for the deuterated and dried samples. All the neutron diffraction peaks of the deuterated samples are shifted to lower angles comparing with the dried samples. This attributes to the expansion of the lattice due to the introduction of oxide and deuterium ions into the dry samples. The location of deuterium was analyzed by Rietveld method and maximum entropy method (MEM). The MEM shows that deuterium exists at 96j site in  $\text{Ba}_3\text{Ca}_{1.18}\text{Nb}_{1.82}\text{O}_{8.73}$ , which leans to the Ca/Nb mixed site, and 12h site in  $\text{Zr}_{0.8}\text{Sc}_{0.2}\text{O}_{2.9}$ , which is similar to that of the other simple perovskite-type proton conductors. The shift of OD groups slightly toward the opposite side of deuterium was observed in both compounds. The location of proton was discussed comparing with the results of *ab-initio* structure calculations. The results of heat capacity measurements are also discussed in terms of the change of the lattice vibrations due to the introduction of oxide and hydrogen ions.

Keywords: neutron diffraction, proton conductivity, *ab-initio* calculations

## P08.14.147

*Acta Cryst.* (2008). A64, C463

### Solution SAXS and NMR on the domain orientation and binding of the components of human BCKD complex

Yu-Shan Huang<sup>1</sup>, Chi-Fon Chang<sup>2</sup>, U-Ser Jeng<sup>1</sup>

<sup>1</sup>National Synchrotron Radiation Research Center, 101 Hsin-Ann Road, Hsinchu Science Park, Hsinchu, N/A, 30076, Taiwan, <sup>2</sup>Genomics Research Center, Academic Sinica, Taipei, 11529, Taiwan, E-mail: jade@nsrrc.org.tw

The mammalian mitochondrial branched-chain- $\alpha$ -ketoacid dehydrogenase (BCKD) complex, containing E1, E2, and E3 subunits, catalyzes the oxidative decarboxylation of branched-chain- $\alpha$ -ketoacids derived from leucine, isoleucine, and valine, hence, gives rise to branched-chain acyl-CoAs. The transacylase subunit (E2) of BCKD complex carries three independently folded domains linked together by flexible loops: the hbLBD (a.a. 1-84), hbSBD (a.a. 104-152), and C-terminal inner-core domain hbICD (aa.168-395). Both hbLBD and hbSBD domains play central roles in substrate channeling and substrate recognition, which functions relate closely to their structures and relative orientations in the BCKD complex. With solution NMR, we have extracted the individual structures of hbLBD and hbSBD domains, respectively. Whereas the tertiary structure of the full di-domain hbDD (aa. 1-168), consisting of hbLBD, hbSBD, and the linker region, in a linear-like arrangement, is resolved for the first time by solution small angle X-ray scattering (SAXS) with the rigid body refinement, based on the two structures of hbLBD and hbSBD individually determined by NMR. Furthermore, SAXS profiles measured for the E1 component before and after its binding to the hbDD, imply that hbLBD is less confined than hbSBD, in the binding. The result helps in differentiating the two interaction modes of hbDD-E1 and hbDD-E3 in the BCKD complex.

Keywords: SAXS, protein complex structure, NMR

## P08.14.148

*Acta Cryst.* (2008). A64, C463-464

### Crystal and local structural studies of superionic conductor cubic CuI

Dyah S. Adipranoto<sup>1</sup>, Masao Yonemura<sup>2</sup>, Kazuhiro Mori<sup>3</sup>, Fumihito Shikanai<sup>1</sup>, Keiji Itoh<sup>3</sup>, Je-Geun Park<sup>4</sup>, Agus Purwanto<sup>5</sup>, Toru Ishigaki<sup>6</sup>, Takashi Kamiyama<sup>1</sup>

<sup>1</sup>High Energy Accelerator Research Organization, Department of Materials Structure Science, dyahs@post.kek.jp, Tsukuba, Ibaraki, 305-0801, Japan, <sup>2</sup>Institute of Applied Beam Science, Ibaraki University, Ibaraki, 316-8511, Japan, <sup>3</sup>Research Reactor Institute, Kyoto University, Osaka, 590-0494, Japan, <sup>4</sup>Department of Physics, Sungkyunkwan University, Korea, <sup>5</sup>Research Center for Nuclear Industrial Materials, BATAN, Indonesia, <sup>6</sup>Frontier Research Center for Applied Nuclear Sciences, Ibaraki University, Ibaraki, 316-8511, Japan, E-mail: dyah.adipranoto@yahoo.com

Crystalline superionic conductor of copper iodide (CuI) with cubic symmetry has been studied by time-of-flight (TOF) neutron powder diffraction in  $\gamma$ -phase (300 K) and  $\alpha$ -phase (773 K). Crystal structure of the both phases were examined by the Rietveld method combined with maximum entropy method (MEM) technique using single-atom and split-atom structural models with the F-43m ( $\gamma$ -phase) and Fm-3m ( $\alpha$ -phase) symmetry, respectively. Local structure analyses were also carried out by employing pair distribution function (PDF) and the reverse Monte Carlo (RMC) techniques to model the disorder of the mobile copper ions. The crystal structure analysis revealed

the temperature dependence of the thermal displacement of the copper ions along the [111] directions, with the average density of copper ions being mostly distributed at the center of tetrahedrally-coordinated I ions. As the ionic conductivity increases in the  $\alpha$ -phase, we found local Cu-Cu correlation evolves with the correlation lengths of 2.47 and 2.72 Å (Fig. 1) rather than the average density distribution shown by the MEM result. These two Cu-Cu correlation lengths roughly correspond to distances between neighboring Cu atoms at the tetrahedral 32f-32f sites and 8c-32f sites in the split-atom model of Fm-3m. We will discuss our results in detail of the high ionic conductivity of  $\alpha$ -phase CuI.

Keywords: superionic conductor, split-atom model, copper iodide

**P08.14.149**

*Acta Cryst.* (2008). A64, C464

**Hysteretic magnetic and dielectric properties in  $\text{Eu}_{1-x}\text{Y}_x\text{MnO}_3$**

Shoichi Danjoh, Hiroyuki Nakamura, Tsuyoshi Kimura  
Osaka university, Graduate school of engineering science, 1-3 Machikaneyama-cho, Toyonaka, Osaka, 560-8531, Japan, E-mail : danjoh@crystal.mp.es.osaka-u.ac.jp

Magnetolectric effects in multiferroics showing both magnetic and ferroelectric orders have been of great interest in recent years. Rare-earth manganites  $\text{RMnO}_3$  with small ionic radii ( $r_R$ ) of R (e.g. R=Tb and Dy) are typical multiferroics, and their ferroelectricity is attributed to magnetic order.  $\text{EuMnO}_3$  with relatively large  $r_R$  shows (weak)-ferromagnetic and paraelectric properties. By doping yttrium into Eu site, however, the ferromagnetic nature disappears while antiferromagnetic ferroelectric feature emerges. Such evolutions of magnetic and electric properties can be tuned by changing the ratio of Eu to Y [1]. In  $\text{Eu}_{1-x}\text{Y}_x\text{MnO}_3$  with  $x \sim 0.2$ , the ferromagnetic paraelectric state competes keenly with the antiferromagnetic ferroelectric state. To examine the competition between the two phases in more detail, we performed measurements of magnetization and electric polarization in various conditions for single crystals of  $\text{Eu}_{1-x}\text{Y}_x\text{MnO}_3$  ( $x \sim 0.2$ ). In this presentation, we will present the observation of characteristic hysteretic behaviors in magnetic and dielectric properties, and discuss the observed results in terms of spatial coexistence of ferromagnetic and ferroelectric phases.

Keywords: magnetic perovskite materials, magnetolectricity, structural and magnetic phase transitions

**P08.14.150**

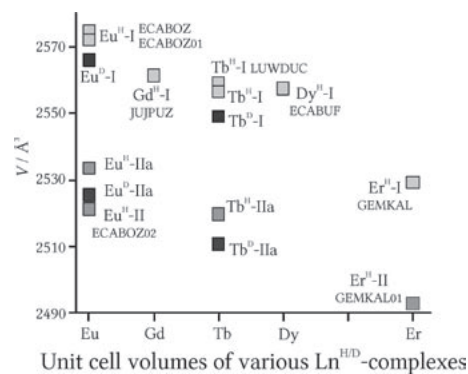
*Acta Cryst.* (2008). A64, C464

**Subtle structural differences in the system  $[\text{Ln}(\text{phen}/\text{phen-d}_8)_2(\text{NO}_3)_3]$  ( $\text{Ln}=\text{Eu}^{3+}, \text{Tb}^{3+}$ )**

Franz Werner<sup>1</sup>, Kentaro Tada<sup>1</sup>, Ayumi Ishii<sup>1</sup>, Hideki Ohtsu<sup>1</sup>, Jungeun Kim<sup>2</sup>, Kenichi Kato<sup>2</sup>, Masaki Takata<sup>2</sup>, Miki Hasegawa<sup>1</sup>  
<sup>1</sup>Aoyama-Gakuin University, College of Science and Engineering, 5-10-1 Fuchinobe, Sagamihara, Kanagawa, 229-8558, Japan, <sup>2</sup>RIKEN/SPring-8, 1-1-1 Kouto, Sayo-cho, Sayo-gun, Hyogo 679-5198, Japan, E-mail : fwerner@mail.zserv.tuwien.ac.at

Recently we compared the structural and electronic behaviour of  $[\text{Pr}(\text{bathophen})_2(\text{NO}_3)_3]$  (bathophen...4,7-diphenyl-1,10-phenanthroline) with those of its parent phase  $[\text{Pr}(\text{phen})_2(\text{NO}_3)_3]$

[1]. In continuation of this study the effect of phen-d<sub>8</sub> (deuterated 1,10-phenanthroline) on the syntheses of the corresponding europium and terbium complexes, for which two ( $\text{Eu}^{\text{II}}$ -I and II) and one ( $\text{Tb}^{\text{II}}$ -I) modification are described in the literature, is reported here. Precipitation from ethanol and ethanol-d<sub>6</sub> yielded powdery samples with unprecedented compositions. Instead of the expected pure modification I in all four cases, phase mixtures of I and a new modification, IIa, were obtained with preference for IIa when hydrogenated phen was used. Although the modifications' II and IIa crystal structures are very similar, it was possible to elaborate on the differences of II/IIa with the help of synchrotron powder data. Additional measurements of the optical emission properties showed a considerable decrease of the quantum yield in the case of the deuterated terbium complex whereas that of the europium complex is slightly increased. [1] Ishii, A. *et al.* (2007), *ChemPhysChem* **8**(9), 1345-1351



Keywords: modification, deuterium effect, luminescence

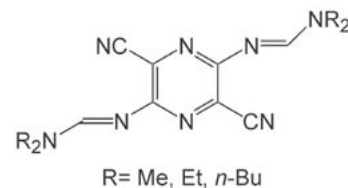
**P08.14.151**

*Acta Cryst.* (2008). A64, C464

**Structure-colour relationship of diaminodicyanopyrazine derivatives having azomethine groups**

Shinya Matsumoto, Atsushi Koseki  
Yokohama National University, Department of Environmental Sciences, Faculty of Education and Human Sciences, 79-2 Tokiwadai, Hodogaya-ku, Yokohama, Kanagawa, 240-8501, Japan, E-mail : smatsu@edhs.ynu.ac.jp

Three diaminodicyanopyrazine dyes with azomethine groups (Figure), which show the same colour in solution, were found to exhibit different colours in single crystals depending on the substituents on the amino groups. In this study, structure-colour relationship in the crystals of these pyrazine dyes was investigated in terms of molecular deformation and an exciton interaction. The difference in molecular conformation was found in the dihedral angles between the pyrazine ring and the azomethine groups. This geometrical feature is well-correlated with the calculated absorption band. This result indicates that the present colour difference in a crystalline state can be ascribed to the influence of molecular deformation. An exciton interaction was also estimated by using an extended-dipole model, but its influence was found to be smaller than the energy shift due to the molecular deformation.



Keywords: functional dyes and polymers, structure-colour relationships, intermolecular interactions